Superexchange in Magnetic Insulators: An Interpretation of the Metal−Metal Charge Transfer Energy in the Anderson Theory

Høgni Weihe*

Institute of Chemistry, University of Copenhagen, Universitetsparken 5, DK-2100 Copenhagen, Denmark

Hans U. Güdel*

Department of Chemistry and Biochemistry, University of Berne, Freiestrasse 3, CH-3000 Berne, Switzerland

Hans Toftlund*

Institute of Chemistry, University of Odense, Campusvej 55, DK-5230 Odense M, Denmark

Received July 1, 1999

The superexchange interactions in four three-center model systems A−L−B, for A and B being paramagnetic centers and L a diamagnetic bridging ligand, are analyzed by valence bond configuration interaction models in combination with fourth-order perturbation theory. We analyze the four distinct cases where a bridging ligand orbital simultaneously interacts with half-filled orbitals localized on A and B (case i), a half-filled orbital localized on A and an empty orbital localized on B (case ii), a full orbital localized on A and a half-filled orbital localized on B (case iii), and finally a full orbital localized on A and an empty orbital localized on B (case iv). In all four cases we compare our new results using localized orbitals with the equivalent results obtained using the Anderson ansatz of delocalized (magnetic) orbitals. The effective metal-to-metal electron transfer energy U_{eff} in the old formalism with delocalized orbitals is expressed in terms of the metal-to-metal electron transfer energy U and the ligand-to-metal electron transfer energy Δ using localized orbitals. We find that the old formalism containing only U_{eff} is in general not sufficient. For cases i and ii we show that U_{eff} can be regarded as an effective U strongly reduced with respect to the free ion as a result of hybridization effects, whereas the same reduction of U for the cases iii and iv is not possible. The relevance and applicability of our theoretical results is demonstrated on magnetochemical data from the literature.

1. Introduction

Understanding the magnetic consequences of weak interactions between paramagnetic metal ions is not only a classical goal in inorganic physical chemistry. It is indeed a prerequisite for an understanding of macroscopic magnetic phenomena and for the design of new magnetic materials.[1,2]

In extended lattices the nearest neighbor interactions are the leading ones. Dimers and higher clusters of magnetic ions can therefore be considered as molecular models for a detailed study of the microscopic magnetic interactions. Cooperative phenomena and more extended interactions do not complicate the situation in these systems, and an analysis in terms of simple molecular models can be done.

Another context in which understanding the magnetic properties of transition metal complexes has gained importance is that of natural enzymatic systems containing paramagnetic metal ions and especially polynuclear transition metal units. Compositional and structural information is contained in a temperature dependent magnetic susceptibility curve of a polynuclear transition metal complex, natural or not. However, a successful extraction of this information heavily depends on whether suitable laboratory-synthesized model systems are available for comparative purposes.[3,4]

The dimer interaction has traditionally been formulated in terms of the Heisenberg−Dirac−van Vleck (HDvV) spin Hamiltonian

$$\hat{H} = J\hat{\mathbf{S}}_{\text{A}}\cdot\hat{\mathbf{S}}_{\text{B}} \tag{1}$$

We are in the following only interested in the ground state magnetic properties. S_{A} and S_{B} are thus the ground state spin values of the paramagnetic metal centers A and B, respectively, and they are both non-zero. Equation 1 leads to a Landé interval splitting of the spin multiplets with $S = S_{\text{A}} + S_{\text{B}}$, $S_{\text{A}} + S_{\text{B}} - 1$, ..., $|S_{\text{A}} - S_{\text{B}}|$. For $J = 0$, these spin multiplets are all degenerate. As defined in eq 1 positive and negative values of the exchange parameter J correspond to antiferromagnetic and ferromagnetic

(1) Gatteschi, D. *Adv. Mater.* **1994**, *6*, 635.
(2) Kahn, O. *Molecular Magnetism*; VCH: New York, 1993.
(3) Hartmann, J. R.; Rardin, R. L.; Chaudhuri, P.; Pohl, K.; Wieghardt, K.; Nuber, B.; Weiss, J.; Papaefthymiou, G. C.; Frankel, R. B.; Lippard, S. J. *J. Am. Chem. Soc.* **1987**, *109*, 7387. Armstrong, W. H.; Spool, A.; Papaefthymiou, G. C.; Frankel, R. B.; Lippard, S. J. *J. Am. Chem. Soc.* **1984**, *106*, 3653.
(4) Weihe, H.; Güdel, H. U. *J. Am. Chem. Soc.* **1997**, *119*, 6539.

10.1021/ic990779h CCC: $19.00
Published on Web 03/09/2000

interaction, respectively, between the centers A and B. J is a parameter to be determined from experiment.

Equation 1 provides an excellent basis for rationalizing bulk properties such as magnetic susceptibility and heat capacity in dimer systems as well as systems with extended interactions. There has therefore been a great effort to interpret the parameter J in eq 1 in terms of more fundamental quantities for the metal pair in question.

Among the models proposed, the Goodenough−Kanamori rules[5−9] are probably the best known. They were formulated as a result of an interplay between experimental studies and theoretical considerations. In short, these rules state that when there is a non-zero one-electron interaction matrix element between orbitals centered on different paramagnetic centers, then this one-electron interaction can lead to an antiferromagnetic or ferromagnetic energy splitting. The magnitude and sign of the contribution to J depends on the filling of the interacting orbitals.[10−12] There are the following four possibilities to consider:

(i) both orbitals are half-filled;

(ii) one orbital is half-filled and the other one is empty;

(iii) one orbital is full and the other one is half-filled;

(iv) one orbital is full and the other one is empty.

If, on the other hand, there is no such one-electron interaction matrix element, the interaction can be ferromagnetic due to a true two-center two-electron exchange integral. There are other contributions to J than the one-electron and two-electron interactions.[11] These are small and will not be considered here.

The conceptual framework to understand the interaction within pairs of paramagnetic ions in insulating lattices was first developed by Anderson.[5,10] A valence bond configuration interaction (VBCI) model expliciely including the bridging ligands was introduced and applied to molecular systems in refs 13 and 14. A splitting of the spin multiplets $S = S_A + S_B$, $S_A + S_B - 1$, ..., $|S_A - S_B|$ from the ground electron configuration, and hence a nonzero J value of eq 1, arises because these spin multiplets can interact with spin multiplets arising from two distinct energetically higher-lying electron configurations.[10] These are first a bridging ligand-to-metal electron transfer (LMCT) and second a metal-to-metal electron transfer (MMCT) electron configuration at energies Δ and U, respectively, relative to the ground state electron configuration. The ground configuration interacts under the action of the one-electron part of the Hamiltonian directly with the LMCT configuration, which in turn interacts with the MMCT configuration. This latter interaction is spin dependent and hence produces a splitting of the spin multiplets arising from the ground electron configuration. In a configuration interaction model this splitting appears on going to fourth order in perturbation theory. Such a perturbational treatment is valid when the parameter V describing the one-electron interaction is much smaller than both U and Δ.

Magnetic insulators can be characterized as being of Mott−Hubbard type ($U < \Delta$) or of charge-transfer type ($\Delta < U$).[15] It has been shown that Anderson's original treatment of the exchange phenomenon only gives a reasonable description of the situation when $U \ll \Delta$.[16] This might be a fair assumption for materials like the divalent titanium and vanadium oxides, in which the band gap is known to be of d−d (MMCT) character.[15] This is also qualitatively easy to understand from a chemical point of view. Ti^{2+} and V^{2+} are both strongly reducing species. This implies that the orbital energies of the valence d orbitals are relatively high compared to the later divalent members of the first transition series, making ligand (oxide) to metal electron transfers high-energy excitations. However, the assumption $U < \Delta$ will certainly break down for most other insulating transition metal compounds in which the metal is less reducing and/or the anion less electronegative.[17] In a reinvestigation of the magnetic properties of the oxides of divalent manganese, iron, cobalt, and nickel,[16] it was concluded that Δ and U in these substances were in the ranges 48400−79800 cm^{-1} and 71000−77400 cm^{-1}, respectively, and hence of equal magnitudes. We conclude that $^1/_2U < \Delta < U$ is a typical range of Δ values relative to U.

The position of the first charge transfer bands in an absorption spectrum of a coordination compound is known to depend strongly on the nature of the ligands as well as the cation.[18] For classical monomeric coordination compounds LMCT bands usually appear in the blue or the near ultraviolet spectral region. This makes $\Delta \approx 30000-40000$ cm^{-1}, and U values are estimated to be typically at least twice this, see above.

We will use the valence bond configuration interaction (VBCI) model as introduced and applied to molecular systems by Solomon and Tuczek.[13,14] We will show that the restriction of one unpaired electron per magnetic center[13] can be overcome and that a similar treatment of cases ii, iii, and iv is justified.

Our paper is organized as follows. In the next section we outline some of the problems which are met when the old formalism for exchange interactions is used to interpret experimental J values. Section 3 gives an introduction to the configuration interaction model and defines the orbitals and one-electron parameters that are used. In section 4 we apply the configuration interaction model to the four above-mentioned cases i−iv in turn. In section 5 we discuss the results and demonstrate their applicability to experimental J values from the literature. The obtained results will allow us to predict which electron configurations can give rise to large ferromagnetic interaction between paramagnetic centers in a solid.

2. The Problems

In this section we briefly outline the commonly used formalism and discuss the model parameters.

We consider a system consisting of two metal centers A and B. Both A and B have their individual environments of nonbridging and bridging ligands. The geometry and symmetry of the system is not relevant at this point.

We are interested in the interaction between the orbitals a_i and b_j centered on the metal centers A and B, respectively. a_i is essentially an antibonding A orbital, i.e., it contains some bridging-ligand character; similarly with orbital b_j. These so-

(5) Anderson, P. W. In *Magnetism*; Rado, G. T., Suhl, H., Eds.; Academic Press: New York, 1963; Vol. 1, Chapter 2.
(6) Goodenough, J. B. *Phys. Rev.* **1955**, *79*, 564.
(7) Goodenough, J. B. *J. Phys. Chem. Solids* **1958**, *6*, 287.
(8) Kanamori, J. *J. Phys. Chem. Solids* **1959**, *10*, 87.
(9) Wollan, E. O.; Child, H. R.; Koehler, W. C.; Wilkinson, M. K. *Phys. Rev.* **1958**, *112*, 1132.
(10) Anderson, P. W. *Phys. Rev.* **1959**, *115*, 2.
(11) Goodenough, J. B. *Magnetism and the Chemical Bond*; Interscience: New York, 1963.
(12) Weihe, H.; Güdel, H. U. *Inorg. Chem.* **1997**, *36*, 3632.
(13) Tuczek, F.; Solomon, E. I. *Inorg. Chem.* **1993**, *32*, 2850.
(14) Brown, C. A.; Remar, G. J.; Musselmann, R. L.; Solomon, E. I. *Inorg. Chem.* **1995**, *34*, 688.
(15) Zaanen, J.; Sawatzky, G. A.; Allen, J. W. *Phys. Rev. Lett.* **1985**, *55*, 418.
(16) Zaanen, J.; Sawatzky, G. A. *Can. J. Phys.* **1987**, *65*, 1262.
(17) Ronda, C. R.; Arends, G. J.; Haas, C. *Phys. Rev. B* **1987**, *35*, 4038.
(18) Jørgensen, C. K. *Prog. Inorg. Chem.* **1970**, *12*, 101.

called magnetic orbitals[19] a_i and b_j are made orthogonal by an orthogonalization process. The reason for this redefinition of the relevant orbitals is simply that the splitting of the spin multiplets arising from the ground electron configuration will now appear already in second order in perturbation theory.

If both a_i and b_j are half-filled (case i), an interaction between a_i and b_j contributes to the J value with[12]

$$J_{\mathrm{i}} = +\frac{4}{n_{\mathrm{A}} n_{\mathrm{B}}}\frac{h_{ij}^2}{U_{\mathrm{eff}}} \tag{2}$$

n_{A} and n_{B} are the total number of unpaired electrons in the ground state of A and B, respectively. h_{ij} is a parameter formally defined as

$$h_{ij} = \langle a_i|\hat{h}|b_j\rangle \tag{3}$$

with $\hat{h}$ the appropriate one-electron interaction Hamiltonian. U_{eff} is the energy difference between the ground electron configuration and an electron configuration in which one electron has been taken from the magnetic orbital a_i and restored in the other magnetic orbital b_j, and vice versa. We distinguish clearly between U and U_{eff} in this paper. U_{eff} is the electron transfer energy appearing in the old formalism with magnetic orbitals, whereas U is the electron transfer energy involving localized metal orbitals with no bridging-ligand character. The relationship between U_{eff} and U will be established below.

If a_i is half-filled and b_j is empty (case ii), we find the following contribution to J:

$$J_{\mathrm{ii}} = -\frac{2}{n_{\mathrm{A}}(n_{\mathrm{B}}+1)}\frac{h_{ij}^2}{U_{\mathrm{eff}}}\frac{I_{n_{\mathrm{B}}+1}}{U_{\mathrm{eff}}} \tag{4}$$

Here we introduced the symbol $I_{n_{\mathrm{B}}+1}$ which accounts for one-center exchange interactions on center B. The ratio $I_{n_{\mathrm{B}}+1}/U_{\mathrm{eff}}$ can be approximated as[12]

$$\frac{I_{n_{\mathrm{B}}+1}}{U_{\mathrm{eff}}} = (n_{\mathrm{B}}+1)\frac{I_{\mathrm{B}}}{U_{\mathrm{eff}}} \tag{5}$$

with I_{B} a constant which is an average one-center exchange integral for center *B*. See refs 12 and 20 for a detailed discussion of this quantity. The average one-center exchange integral is closely related to the spin-pairing energy discussed by Jørgensen.[21]

If a_i is full and b_j is half-filled (case iii), we find the following contribution to J[12]

$$J_{\mathrm{iii}} = -\frac{2}{(n_{\mathrm{A}}+1)n_{\mathrm{B}}}\frac{h_{ij}^2}{U_{\mathrm{eff}}}\frac{I_{n_{\mathrm{A}}+1}}{U_{\mathrm{eff}}} \tag{6}$$

Notice the similarity between equations 4 and 6. Cases ii and iii are particle−hole equivalents as long as we operate with magnetic orbitals only. This is clearly no longer so when the bridging ligands are included. We will show that inclusion of the bridging ligand orbitals will dramatically influence the relative magnitudes of J_{ii} and J_{iii}.

Finally, if a_i is full and b_j is empty (case iv), we find the following contribution to J:[12,22]

$$J_{\mathrm{iv}} = +\frac{2h_{ij}^2}{(n_{\mathrm{A}}+1)(n_{\mathrm{B}}+1)}\frac{2}{U_{\mathrm{eff}}^3} I_{n_{\mathrm{A}}+1} I_{n_{\mathrm{B}}+1} \tag{7}$$

Equations 4, 6, and 7 are all valid when $U_{\mathrm{eff}} \gg I_{n_{\mathrm{A}}+1} I_{n_{\mathrm{B}}+1}$.

Case i has received by far the most attention, and eq 2 has been used for numerous successful analyses of experimental J values of transition metal dimers in which the constituting metal ions are antiferromagnetically coupled.[4,20,23−26] However, in most of these studies, the ratio $h_{ij}^2/U_{\mathrm{eff}}$ has been taken as an effective parameter. No critical analysis of this ratio seems to have been performed. We now list several examples in which the $h_{ij}^2/U_{\mathrm{eff}}$ ratios obtained in this way clearly deviate from h_{ij}^2/U.

The μ-oxo-decaammine-dichromium(III) cation $[(NH_3)_5\text{-}CrOCr(NH_3)_5]^{4+}$ (basic rhodo) has a special place in this context, by having a high symmetry (close to D_{4h}) and having been investigated with several techniques. Temperature dependent magnetic susceptibility measurements[27] as well as optical spectroscopy[28,29] have determined $J \approx 450\ \mathrm{cm}^{-1}$. Due to the high symmetry, the parameter h_{ij} can be related to the e_π ligand field parameter in the angular overlap model (AOM) description[29,30] (see also section 4.1) as follows:

$$h_{ij} = e_\pi \tag{8}$$

Using eq 2 we then obtain[12,20,29,30]

$$J = \frac{8}{9}\frac{e_\pi^2}{U_{\mathrm{eff}}} \tag{9}$$

The AOM parameter e_π is a measure of the π donor strength of the oxide ion as ligand to trivalent chromium. It was estimated in ref 29 to have the value 4000 cm^{-1}, which makes the oxide ion an outstandingly strong π donor compared to other simple ligands. This high value is supported by the analysis of single crystal absorption spectra of oxo coordinated Ni^+ and Ni^{2+} species, in which e_π values of 3000 and 3500 cm^{-1}, respectively, were determined.[31] Inserting $e_\pi = 4000\ \mathrm{cm}^{-1}$ and $J = 450\ \mathrm{cm}^{-1}$ in eq 9 we obtain $U_{\mathrm{eff}} = 31600\ \mathrm{cm}^{-1}$. An upper limit for U, on the other hand, can be estimated from the free ion ionization potentials.[10] This upper limit is for a chromium(III) dimer $U \approx 146300\ \mathrm{cm}^{-1}$ [32] which is obtained as the difference between

(19) Construction of magnetic orbitals in a three-center model system is discussed in some detail by Mayer and Angelov: Mayer, I.; Angelov, S. A. *Int. J. Quantum Chem.* **1980**, *18*, 783.
(20) Weihe, H.; Güdel, H. U. *J. Am. Chem. Soc.* **1998**, *120*.
(21) Jørgensen, C. K. *Modern Aspects of Ligand Field Theory*; North-Holland Publishing Company: Amsterdam, 1971.
(22) An algebraic mistake appears in ref 12 when deriving eq 49 from eqs 41−44. There it was erroneously stated that the contribution to net J was proportional to the difference $I_{n_{\mathrm{A}}+1} - I_{n_{\mathrm{B}}+1}$. In the limit $I_{n_{\mathrm{A}}+1}$, $I_{n_{\mathrm{B}}+1} \ll U_{\mathrm{eff}}$ is proportional to the product $I_{n_{\mathrm{A}}+1} I_{n_{\mathrm{B}}+1}$ as given in eq 7 of the present paper.
(23) Glerup, J.; Hodgson, D. J.; Pedersen, E. *Acta Chem. Scand.* **1983**, *A37*, 161.
(24) Glerup, J.; Goodson, P. A.; Hodgson, D. J.; Michelsen, K. *Inorg. Chem.* **1995**, *34*, 6255.
(25) Lambert, S. L.; Hendrickson, D. N. *Inorg. Chem.* **1979**, *18*, 2683. Lambert, S. L.; Spiro, C. L.; Gagné, R. R.; Hendrickson, D. N. *Inorg. Chem.* **1982**, *21*, 68. See also ref 43.
(26) Hotzelmann, R.; Wieghardt, K.; Flörke, U.; Haupt, H.-J.; Weatherburn, D. C.; Bonvoisin, J.; Girerd, J.-J. *J. Am. Chem. Soc.* **1992**, *114*, 1681.
(27) Pedersen, E. *Acta Chem. Scand.* **1972**, *26*, 333.
(28) Güdel, H. U.; Dubicki, L. *Chem. Phys.* **1974**, *6*, 272.
(29) Glerup, J. *Acta Chem. Scand.* **1972**, *26*, 3775.
(30) Atanasov, M.; Angelov, S. *Chem. Phys.* **1991**, *150*, 383.
(31) Möller, A.; Hitchman, M. A.; Krausz, E.; Hoppe, R. *Inorg. Chem.* **1995**, *34*, 2684. Hitchman, M. A.; Stratemeier, H.; Hoppe, R. *Inorg. Chem.* **1988**, *27*, 2506.
(32) *Handbook of Chemistry and Physics*, 69th ed.; CRC Press: Boca Raton, FL, 1988−1989 (table with ionization potentials).

the fourth and the third ionization potentials of chromium. These values are significantly reduced in a solid or a complex, but even allowing a reduction down to 50−60% of the free-ion value[10] we conclude that the above-calculated U_{eff} value of 31600 cm^{-1} is a factor of 2−3 lower than U, i.e.,

$$\frac{2}{U} < \frac{1}{U_{\text{eff}}} < \frac{3}{U} \tag{10}$$

We note in passing that in $CuCl_4^{2-}$ U has been determined to be ≈53000 cm^{-1},[33] and that the MMCT energy U is expected to increase with oxidation number,[32] thus lending support to the above conclusion. Another semiempirical treatment of the basic rhodo ion[30] inserted an estimated U_{eff} value of 74500 cm^{-1} into eq 9. This led to an e_π value of 6150 cm^{-1}, which is much too high, and has not been supported by independent experiments (see above).

This problem is not specific for the basic rhodo ion. In ref 20 we analyzed experimental J values of linear and bent oxo bridged trivalent transition metal dimers with d^1d^1, d^2d^2, d^2d^3, d^3d^3, d^3d^4(hs), d^3d^5(hs), d^4(hs)d^4(hs), d^4(ls)d^4(ls), d^4(hs)d^5(hs) and d^5(hs)d^5(hs) electron configurations (hs and ls stand for high-spin and low-spin, respectively). The ratios h_{ij}^2/U_{eff} were found to be transferable between the various electron configurations, so we conclude that the problem is a general one.

This conclusion is further supported by a similar investigation of the ratio I/U_{eff} using eq 5 and a comparison with I/U. The theoretical value of the ratio I/U is estimated as follows. I is an average one-center exchange integral which takes the value 4000−5000 cm^{-1} for di- and trivalent 3d transition metals. U values for dimers with trivalent 3d metal ions, as estimated above, are of the order 80000−100000 cm^{-1}. Consequently, I/U values should be of the order $^1/_{20}$ to $^1/_{15}$. In an analysis of the ground state magnetic properties of an extensive series of homo- and heteronuclear oxo bridged 3d transition metal dimers with trivalent metals we found $I/U_{\text{eff}} = {}^1/_4$,[20] a factor of 4−5 bigger than the estimated I/U ratio, i.e.,

$$\frac{4}{U} < \frac{1}{U_{\text{eff}}} < \frac{5}{U} \tag{11}$$

This clearly indicates that the parameter U_{eff} as used in the original Anderson theory must not be equated with the MMCT energy U. The model needs refinement if the model parameters are to be correlated with other physical properties of the system. This will be done in the next sections by explicitly including the relevant orbital on the bridging ligand L.

3. The Model

In our A−L−B three-center system the paramagnetic centers A and B may be identical or they may be different. (a) is a set of pure A orbitals centered on A; similarly with (b). We consider a pure ligand orbital l' centered on L, and this orbital has an overlap S_a with only one orbital a_i centered on A and an overlap S_b with only one orbital b_j centered on B. We define a new "ligand" orbital[13]

$$l = \frac{1}{\sqrt{1 - S_a^2 - S_b^2}}(l' - S_a a_i - S_b b_j) \tag{12}$$

With the definition eq 12 the orbital l is orthogonal to both a_i and b_j. In addition, any orbital in (a) is assumed orthogonal to any orbital in (b). Notice, that we have made no assumption on the nature of the two overlaps S_a and S_b. They can be pure σ- or π-type overlaps, but might as well be a mixture of both due to misoriented orbitals. Similarly, we have made no assumptions about the nature of the a_i and b_j orbitals. They can be valence or core orbitals. We do, however, assume that the bridging ligand has no unpaired electrons, i.e., that the orbital l is doubly occupied in the ground electron configuration of the A−L−B three-center system. Notice that the orbitals (a) and (b) contain no bridging-ligand character, but they might contain nonbridging-ligand character not explicitly included in the description.

The hybridization matrix elements describing the one-electron interaction between A and L and between L and B are in the following designated V_A and V_B, respectively. V_A is formally defined as

$$V_A = \langle l|\hat{h}|a_i\rangle = \frac{1}{\sqrt{1 - S_a^2 - S_b^2}}[\langle l'|\hat{h}|a_i\rangle - S_a\langle a_i|\hat{h}|a_i\rangle - S_b\langle b_j|\hat{h}|a_i\rangle] \tag{13}$$

with $\hat{h}$ being the one-electron part of the Hamiltonian; similarly with V_B. $\hat{h}$ is spin independent; therefore V_A is zero unless the electrons in the orbitals l and a_i have the same spin quantum numbers. Following the approximation by Wolfsberg and Helmholz[34] or Ballhausen and Gray,[35] the first term in the square bracket of eq 13 is proportional to the overlap between the orbitals l' and a_i, namely, S_a. The term $\langle b_j|\hat{h}|a_i\rangle$ is therefore vanishing since b_j and a_i do not overlap. This leads to the simple relationship that V_A is proportional to S_a. Similarily V_B is proportional to S_b.

The key matrix elements to be calculated in the following are of the type

$$\langle S'\Gamma'M_S'M_\Gamma'|\hat{h}|S\Gamma M_S M_\Gamma\rangle \tag{14}$$

where each function is characterized by the spin quantum numbers S and M_S as well as the irreducible representation Γ and its component M_Γ. We will not present a lengthy derivation of a general theory for the computation of this matrix element (cf. ref 12). We generate explicit expressions for the two functions $|S'\Gamma'M_S'M_\Gamma'$ and $|S\Gamma M_S M_\Gamma\rangle$ and then evaluate the matrix element (eq 14). The eigenvalues of the matrixes thus obtained will be examined with nondegenerate perturbation theory up to fourth order.[36]

The basis functions representing the states arising from the electron configuration $(a)^{N_A}(l)^{N_L}(b)^{N_B}$ with N_A, N_L, and N_B being the total number of electrons on A, L, and B, respectively, are generated by applying the following coupling scheme,

$$\{(a)^{N_A}S_A \otimes [(l)^{N_L}S_L \otimes (b)^{N_B}S_B]S_{LB}\}S \tag{15}$$

where we have left out the spatial transformation properties for clarity. In using eq 15 we first take the product in the square bracket to form the intermediate spin S_{LB}. Then we form the $S_A \otimes S_{LB}$ product to obtain the final function with spin quantum number S. The relevant coupling schemes for the cases i−iv are listed in the Appendices A1−A4, respectively.

(33) Didziulis, S. V.; Cohen, S. L.; Gewirth, A. A.; Solomon, E. I. *J. Am. Chem. Soc.* **1988**, *110*, 250.
(34) Wolfsberg, M.; Helmholz, L. *J. Chem. Phys.* **1955**, *23*, 1841.
(35) Ballhausen, C. J.; Gray, H. B. *Inorg. Chem.* **1962**, *1*, 111.
(36) Dalgarno, A. In: *Quantum Theory*; Bates, R. D., Ed.; Academic Press: New York, 1961; Vol. I, p 171.

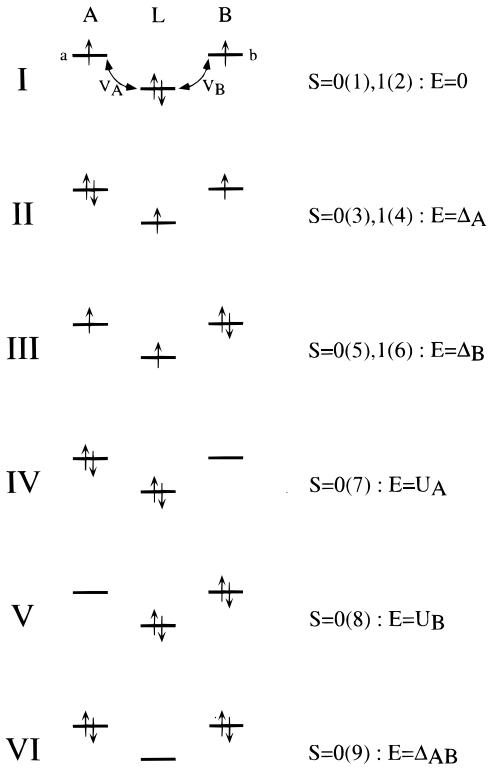

Figure 1. Possible electron configurations for the most simple A−L−B four-electron model (case i). Configuration I represents the ground electron configuration; II and III represent single LMCT electron configurations; IV and V represent MMCT electron transfer configurations; and VI represents a double LMCT electron configuration. The function illustrated for each electron configuration is the highest M_S component of the highest possible spin value. Non-zero hybridization matrix elements V_A and V_B are indicated with double arrows. Possible spin values S and diagonal energies E are given to the right of each configuration. The numbers in parentheses are basis function numbers used in Appendix A1.

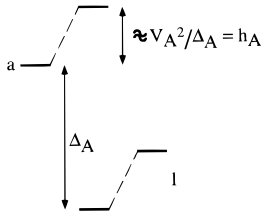

Figure 2. Illustration of the relationship between the h_{ij} parameters of section 2 and the ratio V_A^2/Δ.

4. Results

4.1. J_i: a_i Half-Filled and b_j Half-Filled. Although this case has been discussed by other authors,[13,37,38] we have chosen to include it here in order to illustrate the method, to introduce the approximations, and to illustrate how the parameters h_{ij} in section 2 are related to ligand field parameters.

We consider first the frequently studied three-center four-electron system. Distribution of the four electrons in the three relevant orbitals gives rise to six different electron configurations, see Figure 1. The electron configurations I, II, and III give rise to singlets ($S = 0$) as well as triplets ($S = 1$), whereas IV, V, and VI give rise to singlets only due to the Pauli exclusion principle. Since we do not take into account two-center two-electron exchange integrals, the singlet and triplet states arising from configuration I are degenerate in the absence of an interaction, i.e., for $V_A = V_B = 0$. The same applies for the singlets and triplets arising from II and III.

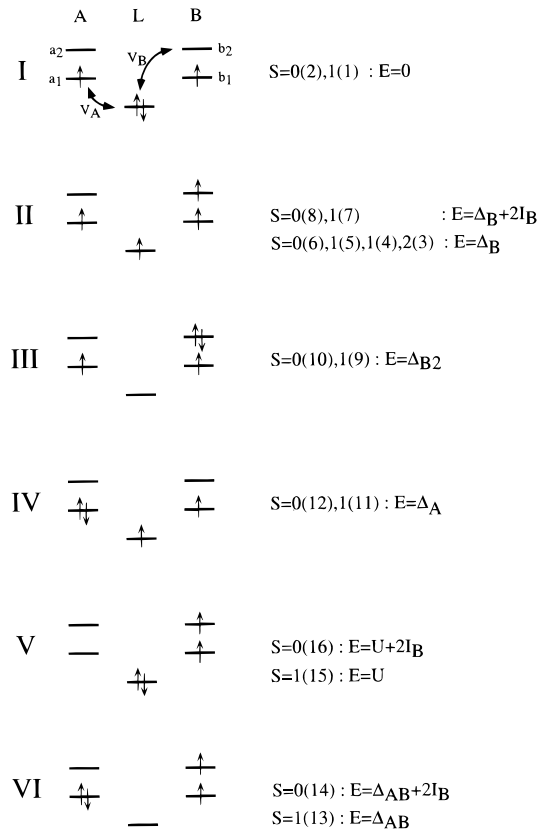

Figure 3. The relevant electron configurations for case ii where the ligand orbital interacts with a half-filled orbital on A and an empty orbital on B. Configuration I represents the ground electron configuration. Configurations II and IV are single LMCT configurations. III and VI are double LMCT configurations, and V is a MMCT configuration. Non-zero hybridization matrix elements V_A and V_B are indicated with double arrows. Possible spin values S and diagonal energies E for each configuration are given to the right. The numbers in parentheses refer to the basis functions used in Appendix A2.

The interaction matrices for the singlet and triplet states are given in eq 43 and 44 in Appendix A1, respectively. The splitting of the lowest-energy triplet and singlet is given by application of fourth-order perturbation theory as

$$E(1) - E(0) = V_A^2 V_B^2 \left[\frac{2}{\Delta_B^2 U_B} + \frac{2}{\Delta_A^2 U_A} + \frac{2}{\Delta_B^2 \Delta_{AB}} + \frac{2}{\Delta_A^2 \Delta_{AB}} + \frac{4}{\Delta_A \Delta_B \Delta_{AB}}\right] \quad (16)$$

As defined in Figure 1, the quantities Δ_A and Δ_B correspond to LMCT and the quantities U_A and U_B to MMCT excitation energies. Δ_{AB} corresponds to a double LMCT excitation. We now introduce the approximations $\Delta_A = \Delta = \Delta_B$ and $U_A = U = U_B$, which are valid if A and B are identical. We thus obtain

$$E(1) - E(0) = 4\frac{V_A^2}{\Delta}\frac{V_B^2}{\Delta}\left[\frac{1}{U} + \frac{2}{\Delta_{AB}}\right] \quad (17)$$

which is valid for this particular four-electron system, i.e., for $n_A = n_B = 1$.

We also performed calculations for model systems with the ground electron configuration $(a)^{n_A}(l)^2(b)^{n_B}$ with n_A and/or n_B

(37) Geertsma, W. *Physica B* **1990**, *164*, 241.
(38) Shen, Z.; Allen, J. W.; Yeh, J. J.; Kang, J.-S.; Ellis, W.; Spicer, W.; Lindau, I.; Maple, M. B.; Dalichaouch, Y. D.; Torikachvili, M. S.; Sun, J. S.; Geballe, T. H. *Phys. Rev B* **1987**, *36*, 8414.

different from 1. The general expression for the contribution to J is

$$J_i = \frac{4}{n_A n_B}\frac{V_A^2}{\Delta}\frac{V_B^2}{\Delta}\left[\frac{1}{U}+\frac{1}{\Delta}\right] \tag{18}$$

where we have assumed $\Delta_{AB} = 2\Delta$.[14,37] Notice that there will be no splitting unless both one-electron interaction matrix elements V_A and V_B are non-zero.

If the energy difference between the metal and the ligand orbital is the main contribution to the LMCT energy Δ, then the factor V_A^2/Δ can be identified as the second-order energy shift of orbital a_i due to the presence of the ligand. The ratios V_A^2/Δ and, similarly, V_B^2/Δ are thus closely related to a ligand field parameter, see Figure 2.

4.2. J_{ii}: a_i Half-Filled and b_j Empty. Now the ligand orbital l' has non-zero overlaps with the half-filled a_1 orbital on A and the empty b_2 orbital on B. The six relevant electron configurations are illustrated in Figure 3. Apart from the ground electron configuration we have only included single and double LMCT and MMCT configurations.

The situation here is slightly more complicated than in the previous section, since we now have the possibility to generate excited configurations with two unpaired electrons on center B, see configurations II, V, and VI in Figure 3. We thus have to include one-center two-electron exchange integrals. The diagonal energies of the spin multiplets arising from the configurations II, V, and VI are determined as follows. We take configuration II as an example. The subconfiguration $b_1^1 b_2^1$ gives rise to a singlet and a triplet. Due to Hund's rule the triplet is lower in energy. The separation between the singlet and the triplet is $2I_B$ where I_B is the exchange integral involving the orbitals b_1 and b_2. The possible spin values S for the total configuration $a_1^1 l^1 b_1^1 b_2^1$ are obtained by inspection of the following series of products,

$$\{(a_1^1)S_A \otimes [(l^1)S_L \otimes (b_1^1 b_2^1)S_B]S_{LB}\}S \tag{19}$$

with $S_A = {}^1/_2$, $S_L = {}^1/_2$, and $S_B = 0$ or 1. All spin multiplets S obtained for $S_B = 0$ are degenerate and similarly with the spin multiplets obtained with $S_B = 1$. This degeneracy is retained because we neglect two-center two-electron exchange integrals.

The configuration interaction matrices for the singlets and triplets are given in eq 46 and 47 in Appendix A2, respectively. After applying fourth-order perturbation theory we find the following energy difference between the lowest triplet and singlet:

$$E(1) - E(0) = -V_A^2 V_B^2\left[\frac{1}{\Delta_B^2 U} - \frac{1}{(\Delta_B + 2I_B)^2(U + 2I_B)} + \frac{2}{\Delta_B\Delta_{AB}\Delta_A} - \frac{2}{(\Delta_B + 2I_B)(\Delta_{AB} + 2I_B)\Delta_A} + \frac{1}{\Delta_B^2\Delta_{AB}} - \frac{1}{(\Delta_B + 2I_B)^2(\Delta_{AB} + 2I_B)} + \frac{1}{\Delta_A^2\Delta_{AB}} - \frac{1}{\Delta_A^2(\Delta_{AB} + 2I_B)}\right] \tag{20}$$

This result is specific for A and B each having one unpaired electron, i.e., $n_A = n_B = 1$. The general expression for the contribution to J of this type of interaction is

$$J_{ii} = -\frac{2}{n_A(n_B+1)}V_A^2 V_B^2\left[\frac{1}{\Delta_B^2 U} - \frac{1}{(\Delta_B + I_{n_B+1})^2(U + I_{n_B+1})} + \frac{2}{(\Delta_B\Delta_{AB}\Delta_A} - \frac{2}{(\Delta_B + I_{n_B+1})(\Delta_{AB} + I_{n_B+1})\Delta_A} + \frac{1}{\Delta_B^2\Delta_{AB}} - \frac{1}{(\Delta_B + I_{n_B+1})^2(\Delta_{AB} + I_{n_B+1})} + \frac{1}{\Delta_A^2\Delta_{AB}} - \frac{1}{\Delta_A^2(\Delta_{AB} + I_{n_B+1})}\right] \tag{21}$$

$I_{n_B+1} = (n_B + 1)I_B$ accounts for the intra-atomic exchange interaction on center B.

It is interesting to note that the double LMCT configuration III at energy Δ_{B2} in Figure 3 does not contribute to the splitting to this order of perturbation theory. The reason for this is that this electron configuration only involves center B and not both centers. The quantities Δ_A, Δ_B, Δ_{AB}, U, and I_B are all positive. Consequently, the content of the square brackets in eq 20 is positive leading to a negative J_{ii}. If the double LMCT configuration VI at energy Δ_{AB} was not included in the model, the content of the square brackets would be reduced to the first two terms.

In order to discuss in simple terms the importance of configuration VI in the model, we first assume $\Delta_{AB} = \Delta_A + \Delta_B$ and $I_{n_B+1} \ll U$, Δ_A, Δ_B.[39] Equation 21 then becomes

$$J_{ii} = -\frac{2}{n_A(n_B+1)}V_A^2 V_B^2\left[\frac{2U + \Delta_B}{\Delta_B^3 U^2} + \frac{4\Delta_B + 2\Delta_A}{\Delta_B^2\Delta_A(\Delta_B + \Delta_A)^2} + \frac{3\Delta_B + 2\Delta_A}{\Delta_B^3(\Delta_B + \Delta_A)^2} + \frac{1}{\Delta_A^2(\Delta_B + \Delta_A)^2}\right] I_{n_B+1} \tag{22}$$

With the assumption $\Delta_A = \Delta_B = \Delta$ we get

$$J_{ii} = -\frac{2}{n_A(n_B+1)}\frac{V_A^2}{\Delta}\frac{V_B^2}{\Delta}\left[\frac{2U+\Delta}{\Delta U^2} + \frac{3}{\Delta^2}\right] I_{n_B+1} \tag{23}$$

The effect of including configuration VI in the model is condensed in the second term in the square brackets of equation 23.

4.3. J_{iii}: a_i Full and b_j Half-Filled. Now the ligand orbital l' interacts with a full orbital on A and a half-filled orbital on B. The relevant electron configurations and their diagonal energies are given in Figure 4. There are only three possible electron configurations. In particular, it is not possible to generate a double LMCT configuration. The configuration interaction matrices for the singlet and triplet states are given in eqs 49 and 50, respectively, of Appendix A3. After applying fourth-order perturbation theory we find the following energy difference between the lowest triplet and singlet:

$$E(1) - E(0) = -\frac{V_A^2}{\Delta}\frac{V_B^2}{\Delta}\left[\frac{1}{U} - \frac{1}{U + 2I_A}\right] \tag{24}$$

This result is specific for A and B each having one unpaired electron, i.e., $n_A = n_B = 1$. The general expression for the contribution of this type of interaction to J is

$$J_{iii} = -\frac{2}{(n_A+1)n_B}\frac{V_A^2}{\Delta}\frac{V_B^2}{\Delta}\left[\frac{1}{U} - \frac{1}{U + I_{n_A+1}}\right] \tag{25}$$

(39) The quality of the assumption $I_{n_k+1} \ll U$ (k = A or B) was discussed in ref 12. Referring to eq 5 of the present paper we see that I_{n_k+1} increases with n_k. The quality of this assumption hence gets worse with increasing n_k.[12] The same is true for the assumptions $I_{n_k+1} \ll \Delta_A$ and $I_{n_k+1} \ll \Delta_B$.

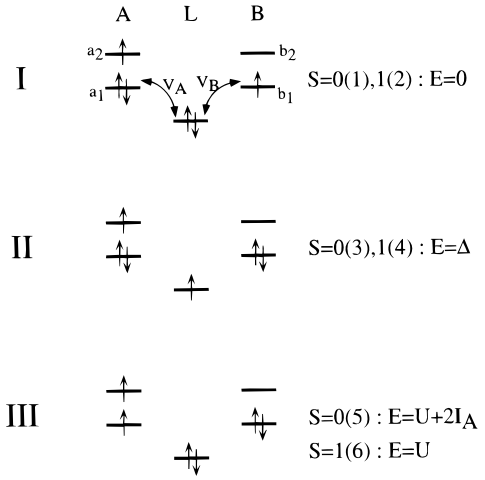

Figure 4. All the possible electron configurations for case iii where the ligand orbital interacts with a full orbital on A and a half-filled orbital on B. Configurational I is the ground electron configuration; II and III are LMCT and MMCT configurations, respectively. Non-zero hybridization matrix elements V_A and V_B are indicated with double arrows. Possible spin values S and diagonal energies E are given to the right of each configuration. The numbers in parentheses refer to the basis functions used in Appendix A3.

Since U and I_{n_A+1} are both positive, the content of the square brackets is positive. J_{iii} is therefore negative. Assuming $I_{n_A+1} \ll U$, eq 25 simplifies to

$$J_{iii} = -\frac{2}{(n_A+1)n_B}\frac{V_A^2}{\Delta}\frac{V_B^2}{\Delta}\frac{I_{n_A+1}}{U^2} \qquad (26)$$

4.4. J_{iv}: a_i Full and b_j Empty. Now the ligand orbital l' interacts with the full orbital a_1 and the empty orbital b_2. The relevant electron configurations and their diagonal energies are given in Figure 5. Notice that it is not possible to generate a double LMCT configuration which involves both paramagnetic centers. The configuration interaction matrices for the singlet and triplet states are given in eqs 52 and 53, respectively, of Appendix A4. After applying fourth-order perturbation theory we find the following energy difference between the lowest triplet and singlet states:

$$E(1) - E(0) = {}^1/_2 V_A^2 V_B^2\left[+\frac{1}{V_B^2 U} + \frac{1}{(\Delta_B+2I_B)^2(U+2I_A+2I_B)} - \frac{1}{\Delta_B^2(U+2I_A)} - \frac{1}{(\Delta_B+2I_B)^2(U+2I_B)}\right] \qquad (27)$$

This result is specific for A and B each having one unpaired electron, i.e., $n_A = n_B = 1$. The general expression for the contribution of this type of interaction to J is

$$J_{iv} = \frac{2}{(n_A+1)(n_B+1)}V_A^2 V_B^2\left[+\frac{1}{\Delta_B^2 U} + \frac{1}{(\Delta_B + I_{n_B+1})^2(U + I_{n_A+1} + I_{n_B+1})} - \frac{1}{\Delta_B^2(U+I_{n_A+1})} - \frac{1}{(\Delta_B+I_{n_B+1})^2(U+I_{n_B+1})}\right] \qquad (28)$$

An analysis of the content of the square brackets of eq 28 reveals that it is positive resulting in a positive J_{iv}. The double LMCT configuration III in Figure 5 involves only one paramagnetic center and therefore does not contribute to J_{iv} to this order of perturbation theory, cf. section 4.2. In the limit $I_{n_A+1}, I_{n_B+1} \ll \Delta_B, U$, eq 28 reduces to

$$J_{iv} = \frac{2}{(n_A+1)(n_B+1)}\frac{V_A^2}{\Delta}\frac{V_B^2}{\Delta}\left[\frac{2}{U^3}+\frac{4}{\Delta U^2}\right]I_{n_A+1}I_{n_B+1} \qquad (29)$$

where we have written $\Delta_B = \Delta$.

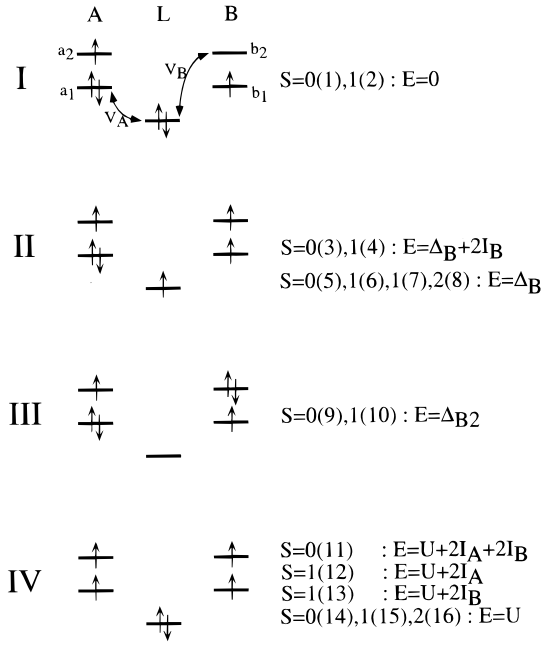

Figure 5. The relevant electron configurations for case iv where the ligand orbital interacts with a full orbital on A and an empty orbital on B. Configuration I represents the ground electron configuration. The configurations II, III, and IV represent single LMCT, double LMCT and MMCT electron configurations, respectively. Non-zero hybridization matrix elements V_A and V_B are indicated with double arrows. Possible spin values S and diagonal energies are given to the right of each configuration. The numbers in parentheses refer to the basis function numbers used in Appendix A4.

5. Discussion

Equations 18, 23, 26, and 29 are the main results of this paper and form the basis of the following discussion.

It is important to realize that in all four cases it is possible to express the contribution to J in terms of the number of unpaired electrons n (n_A, n_B), the hybridization matrix elements V (V_A, V_B), the LMCT energy Δ (Δ_A, Δ_B), and the MMCT energy U (U_A, U_B). While J is a property of the whole system, the parameters n, V, Δ, and U represent properties of elements of the dimer. n is obviously a single-center property. V and Δ are properties of a specified metal−ligand combination. The magnitude of Δ can be obtained by studying LMCT transitions in absorption spectra of mononuclear complexes, and V^2/Δ can be obtained from the study of d−d transitions in the case of transition metal complexes. When A and B are identical, U is a single-ion property. U then corresponds to the difference between two ionization potentials. When A and B are different, U corresponds to the difference between an ionization potential of one center and an electron affinity of the other. U can be experimentally obtained from photoelectron spectra.[33,40−42]

(40) Fujimori, A.; Saeki, M.; Kimizuka, N.; Taniguchi, M.; Suga, S. *Phys. Rev. B.* **1986**, *34*, 7318.

Table 1. Summary of the F_a, G_a, H_a, and K_a Factors as Found in Section 4 and Discussed in Section 5[a]

J_a	$F_a(n_A,n_B)$	$G_a(V_A,V_B,\Delta)$	$H_a(U,\Delta)$	$K_a(I_A,I_B)$	$J_{a,\mathrm{old}}$
J_i	$\frac{4}{n_A n_B}$	$\frac{V_A^2}{\Delta}\frac{V_B^2}{\Delta}$	$\frac{1}{U}+\frac{1}{\Delta}$	1	$\frac{4}{n_A n_B}h^2\frac{1}{U_{\mathrm{eff}}}$
J_{ii}	$\frac{2}{n_B}$	$\frac{V_A^2}{\Delta}\frac{V_B^2}{\Delta}$	$\frac{2U+\Delta}{\Delta U^2}+\frac{3}{\Delta^2}$	I_B	$\frac{2}{n_B}h^2\frac{1}{U_{\mathrm{eff}}^2}I_B$
J_{iii}	$\frac{2}{n_A}$	$\frac{V_A^2}{\Delta}\frac{V_B^2}{\Delta}$	$\frac{1}{U^2}$	I_A	$\frac{2}{n_A}h^2\frac{1}{U_{\mathrm{eff}}^2}I_A$
J_{iv}	2	$\frac{V_A^2}{\Delta}\frac{V_B^2}{\Delta}$	$\frac{2}{U^3}+\frac{4}{\Delta U^2}$	$I_A I_B$	$h^2\frac{2}{U_{\mathrm{eff}}^3}I_A I_B$

[a] The last column gives the old formulas as summarized in section 2. We used the approximation $I_{n_j+1}=(n_j+1)I_j$ (j = A or B) eq 5 to obtain the columns with F_a, K_a, and $J_{a,\mathrm{old}}$.

The equations 18, 23, 26, and 29 are all composed as a product of four factors as follows:

$$J_a = F_a(n_A,n_B)G_a(V_A,V_B,\Delta)H_a(U,\Delta)K_a(I_A,I_B) \qquad (30)$$

with a = i, ii, iii, or iv. Table 1 summarizes the equations in terms of these factors.

5.1. The Principal Factors in the Expressions of *J*. The influence of the number of unpaired electrons on A and B is given in the factors F_a (a = i, ii, iii, and iv) of Table 1. The n_A, n_B dependence of J_i, J_{ii}, J_{iii}, and J_{iv} found here agrees with what has been found earlier.[12] For A and B both being transition metals, the factor F_i can vary by as much as a factor of 25, from 4 to $^4/_{25}$ for $n_A = n_B = 1$ and $n_A = n_B = 5$, respectively. The n_A, n_B dependency of J_i is experimentally very well verified for several series of dimers in which there is only one dominant interaction pathway.[12,20,24] The agreement is not as good when there are several important interaction pathways.[25,43]

As a result of the approximations made in the previous four sections, the factors $G_a(V_A,V_B,\Delta)$ are identical for all a = i, ii, iii, and iv. $G_a(V_A,V_B,\Delta)$ equals a product of the two factors V_A^2/Δ and V_B^2/Δ which are related to ligand field parameters, see section 4.1 and Figure 2. The form of G_a also explains why ligand field models formulated in terms of the angular overlap model have been successful in interpreting magnetic properties of structurally related complexes, e.g., dihydroxo bridged copper(II) dimers and hydroxo bridged chromium(III) dimers.[23,44] The factor G_a immediately tells us which ligand and metal orbitals significantly contribute to the J value and which ones do not. For V_A^2/Δ to have an appreciable value, both metal and ligand orbitals must be valence orbitals, corresponding to the lowest value of Δ. Usage of this principle to vary the magnetic ordering temperature of $Cs_2Mn^{II}[V^{II}(CN)_6]\cdot H_2O$, $CsMn^{II}[Cr^{III}(CN)_6]$, and $Mn^{II}[Mn^{IV}(CN)_6]\cdot xH_2O$ was discussed in ref 45. Core orbitals on the ligand and higher-than-valence orbitals on the metal can usually be neglected, since for these combinations Δ becomes very large and V_A^2/Δ vanishes. Ligand field parameters are roughly constant for isostructural series of homovalent transition metal complexes.[21] This means that the ligand field parameter V_A^2/Δ, if known for a given metal−ligand combination, can be transferred to another homovalent metal with the same ligand.[20] Ligand field parameters increase strongly on increasing the oxidation number[21] due to a lowering of the metal orbitals and thus a decrease of Δ. Similarly, they increase dramatically on moving down a group in the periodic table. This is so because 4d and 5d orbitals are more diffuse than 3d orbitals, giving rise to higher hybridization matrix elements V_A and/or V_B, see eq 13. In the simple case of $V_A = V_B$ and $S_a = S_b$, J will be proportional to the fourth power of the metal−ligand overlap S_a, since V_A is proportional to S_a. This has been found to be valid using ab initio calculations.[46,47]

The factors $H_a(U,\Delta)$ correspond to the factors $1/U_{\mathrm{eff}}$, $1/U_{\mathrm{eff}}^2$, $1/U_{\mathrm{eff}}^2$, and $1/U_{\mathrm{eff}}^3$ in the old model, see last column in Table 1. From Table 1 we see that in the Anderson limit, i.e., $\Delta \gg U$, U_{eff} equals U for all cases. In the Introduction it was shown that $^1/_2U < \Delta < U$ is a physically typical range of relative Δ and U values. We obtain the following ranges of the H_a factors which are compared with the corresponding values in the old model:

new model	old model	
$\frac{2}{U} < H_i < \frac{3}{U}$	$H_i = \frac{1}{U_{\mathrm{eff}}}$	(31)
$\frac{6}{U^2} < H_{ii} < \frac{17}{U^2}$	$H_{ii} = \frac{1}{U_{\mathrm{eff}}^2}$	(32)
$H_{iii} = \frac{1}{U^2}$	$H_{iii} = \frac{1}{U_{\mathrm{eff}}^2}$	(33)
$\frac{6}{U^3} < H_{iv} < \frac{10}{U^3}$	$H_{iv} = \frac{1}{U_{\mathrm{eff}}^3}$	(34)

We note that the ratio U_{eff}/U is different for the four cases, ranging from a minimum of approximately $^1/_4$ in case ii to $^1/_1$ in case iii. For case i the reduction of U_{eff} vs U is solely due to the inclusion of the double LMCT configuration in the model, see section 4.1. For case ii there is already a reduction (first term of H_{ii} in Table 1) without including double LMCT configurations in the model. The second term of H_{ii} expresses the effect of double LMCT configurations and leads to further reduction. For case iii $U_{\mathrm{eff}} = U$, since it is not possible to generate double LMCT configurations. The slight reduction for case iv simply results from the perturbational treatment.

The K_a factors in Table 1 express the intra-atomic exchange interactions on the centers A and B. The K_a factor is different from unity when it is possible to add an electron into the relevant empty orbital or remove an electron from the relevant full orbital on either of the two paramagnetic centers. Therefore, J_i is independent of I_A and I_B. J_{ii} and J_{iii} depend on I_B and I_A, respectively, and J_{iv} depends on the product of I_A and I_B.

(41) van der Laan, G.; Westra, C.; Haas, C.; Sawatzky, G. A. *Phys. Rev. B* **1981**, *23*, 4369.
(42) Sangaletti, L.; Parmigiani, F.; Ratner, E. *Phys. Rev. B* **1998**, *57*, 10175.
(43) Kahn, O. *Struct. Bonding* **1987**, *68*, 89.
(44) Bencini, A.; Gatteschi, D. *Inorg. Chim. Acta* **1978**, *31*, 11.
(45) Entley, W. R.; Girolami, G. S. *Science* **1995**, *268*, 397. The metal orbitals having π symmetry with respect to the $Mn^{II}-CN-M^{n+}$ (M^{n+} = V^{2+}, Cr^{3+}, Mn^{4+}) axis interact via an empty π^* orbital on the cyanide ion. These systems hence have the ground electron configuration $[t_{2g}^3 e_g^2][(\pi^*)^0][t_{2g}^3]$. This is a hole−particle equivalent of case i and can therefore be treated as such.
(46) Hart, J. R.; Rappé, A. K.; Gorun, S. M.; Upton, T. H. *Inorg. Chem.* **1992**, *31*, 5254. See also: Hart, J. R.; Rappé, A. K.; Gorun, S. M.; Upton, T. H. *J. Phys. Chem.* **1992**, *96*, 6255.
(47) Schrivastava, K. N.; Jaccarino, V. *Phys. Rev. B* **1976**, *13*, 299.

The magnitude of the H_a and K_a factors in Table 1 cannot be directly compared since they have different units for the different cases. However, we can compare the relative magnitudes of the products $H_a(U,\Delta) \times K_a(I_A,I_B)$. We choose U between 50000 and 100000 cm^{-1} (roughly 6−10 eV) and let Δ take values within $^1/_2U < \Delta < U$. I_A and I_B are in the interval from 4000 to 5000 cm^{-1}, which is a reasonable estimate for 3d transition metal ions.[12] Using these values we find the products H_aK_a in the following intervals:

$$200 < H_iK_i \times 10^7\ cm^{-1} < 600 \quad (35)$$

$$24 < H_{ii}K_{ii} \times 10^7\ cm^{-1} < 340 \quad (36)$$

$$4 < H_{iii}K_{iii} \times 10^7\ cm^{-1} < 20 \quad (37)$$

$$1 < H_{iv}K_{iv} \times 10^7\ cm^{-1} < 20 \quad (38)$$

The left and right numbers are the values for $(U, \Delta, I) = (100000\ cm^{-1}, 100000\ cm^{-1}, 4000\ cm^{-1})$ and $(U,\Delta,I) = (50000\ cm^{-1}, 25000\ cm^{-1}, 5000\ cm^{-1})$, respectively. This allows us to determine the relative importance of the different contributions J_i, J_{ii}, J_{iii}, and J_{iv} to J:

$$J_i > |J_{ii}| \gg |J_{iii}| > J_{iv} \quad (39)$$

This is at variance with the discussion of these terms in the earlier literature[11] using the U_{eff} formalism. There it was concluded that the terms J_{ii} and J_{iii} were equal and both of minor importance compared with J_i. J_{iv} appears to be ferromagnetic in the older literature,[5] but we find it to be antiferromagnetic. We find that $|J_{ii}|$ is smaller but of the same order of magnitude as J_i. $|J_{ii}|$ is an order of magnitude bigger than $|J_{iii}|$, which again is bigger than but of the same order of magnitude as J_{iv}.

5.2. Comparison with Experiments. Now we relate our findings to experimental J values and their interpretations in the literature. We comment on the four types of contributions J_{iv}, J_{iii}, J_{ii}, and J_i to J in order of increasing importance.

***J*$_{iv}$.** It is indeed justified to check the order of magnitude of the contribution J_{iv} to net J, since this term is always present. The constituting metals in a dimer always possess filled and empty orbitals. The filled orbitals can be either valence or core orbitals, and the empty orbitals can be either valence or higher-than-valence orbitals. However, the contribution of J_{iv} to J is vanishing due to the H_{iv} factor. This term has therefore never been recognized as important in analyses of experimental J values.

***J*$_{iii}$.** It has been argued[48] that the ferromagnetic nearest-neighbor (90°) interaction in NiO results from covalency effects, i.e., the one-electron interactions discussed in the present paper. This is in contrast to the traditional approach where this effect is ascribed to potential exchange.[11] Ni^{2+} is a d^8 electron system which in octahedral symmetry has the ground electron configuration $t_{2g}^6 e_g^2$. Hence, a ferromagnetic interaction of type J_{iii} between the Ni^{2+} ions can arise, if there exist ligand orbitals which are simultaneously overlapping with the filled t_{2g} orbitals on one metal and the half-filled e_g orbitals on the other metal. This is the case for the 90° interaction,[30] and using eq 26 we find that the ferromagnetic contribution to $J(90°)$ is

$$J_{iii} = -2\left(\frac{2}{2}\frac{V_{\sigma p}^2}{\Delta}\frac{V_{\pi p}^2}{\Delta}\right)\frac{1}{U^2}I \quad (40)$$

$V_{\sigma p}$ and $V_{\pi p}$ are the one-electron parameters relevant for the $p\sigma-d\sigma$ and $p\pi-d\pi$ interactions, respectively. Using parameter values from ref 16, 1.6 eV $< V_{\sigma p} <$ 1.9 eV, $V_{\pi p} = {}^1/_2V_{\sigma p}$, $\Delta =$ 6 eV, $U =$ 9.5 eV, and $I =$ 0.5 eV,[12] we find that $-4\ cm^{-1} > J_{iii} > -8\ cm^{-1}$. This compares well with $J(90°) = -10\ cm^{-1}$ as found in ref 49. There are also antiferromagnetic contributions (J_i) to net J in this system.[30] These involve the s orbitals on the oxide ions and are therefore expected to be small, since the 2s orbital is lower in energy by 16 eV[50] than the 2p orbitals. Ab initio calculations[51] on di-oxo bridged nickel complexes have indicated that the relevant two-center exchange integrals in this system vary from 1 cm^{-1} for unperturbed localized d orbitals to 10 cm^{-1} for orbitals which are allowed to delocalize onto the bridging ligand. We conclude that J_{iii} substantially contributes to the ferromagnetic interaction between nearest neighbors in NiO. This is in agreement with ref 48.

***J*$_{ii}$.** Our theoretical finding from eqs 35−38 that $|J_{ii}|$ is an order of magnitude bigger than $|J_{iii}|$ eqs 36 and 37, and comparable in magnitude with J_i for low U and Δ values is new and important. It can be shown that this theoretical result is also experimentally verified. Recently[20] we analyzed experimental J values of a series of bent oxo bridged dimers with the electron configurations d^1d^1, d^2d^2, d^2d^3, d^3d^3, d^3d^4(hs), d^3d^5(hs), d^4(hs)d^4(hs), d^4(hs)d^5(hs), and d^5(hs)d^5(hs) in terms of the old U_{eff} formalism. Since these *d* electron configurations represent empty and half-filled d orbitals only, eqs 2 and 4 were used in the analysis with h_{ij}^2/U_{eff} and I/U_{eff} as independent parameters. We argue in section 2 of the present paper that U_{eff}, as calculated from the experimentally determined h_{ij}^2/U_{eff} and I/U_{eff}, is significantly smaller than any reasonable estimate of U. We now show that this is indeed expected. From the ratios h_{ij}^2/U_{eff} and I/U_{eff} we estimated that $2/U < 1/U_{eff} < 3/U$ and $4/U < 1/U_{eff} < 5/U$, respectively. Combining these estimates we find $8/U^2 < 1/U_{eff}^2 < 15/U^2$, which is in perfect agreement with $6/U^2 < 1/U_{eff}^2 < 17/U^2$ obtained independently, eq 32. This clearly tells us that the parameter values of ref 20 are reasonable.

***J*$_i$.** We finally return to J_i and apply it to the basic rhodo problem mentioned in section 2. We saw in the Introduction that the old formalism based on U_{eff} only provides a qualitative picture of the situation.[16] Equation 18 applied to the ground state of the basic rhodo has the form

$$J_i = 2 \times \frac{4}{3\cdot 3}\frac{V_{p\pi}^2}{\Delta}\frac{V_{p\pi}^2}{\Delta}\left(\frac{1}{U}+\frac{1}{\Delta}\right) \quad (41)$$

$$= \frac{8}{9}e_\pi^2\left(\frac{1}{U}+\frac{1}{\Delta}\right) \quad (42)$$

For e_π and U we use the values 4000 cm^{-1} [29] and 74500 cm^{-1},[30] respectively, see also section 2. We estimate the oxide-to-chromium LMCT energy Δ from single crystal spectra of corundum doped with Cr^{3+}.[52,53] Oxide to chromium electron transfer transitions start at 42000 cm^{-1},[52] and an intense band was found at 56000 cm^{-1}.[53] Using $e_\pi = 4000\ cm^{-1}$, $U = 74500\ cm^{-1}$, and $42000\ cm^{-1} < \Delta < 56000\ cm^{-1}$, we find that $445\ cm^{-1} < J < 530\ cm^{-1}$ for the basic rhodo ion. This is in excellent agreement with the experimentally determined value of $J = 450\ cm^{-1}$.[27−29] We note in passing that an intense band

(48) Oguchi, T.; Terakura, K.; Williams, A. R. *Phys. Rev. B* **1983**, *28*, 6443.
(49) Hutchings, M. T.; Samuelson, E. J. *Solid State Commun.* **1971**, *9*, 1011.
(50) Fujimori, A.; Minami, F. *Phys. Rev. B* **1984**, *30*, 957.
(51) Wang, C.; Fink, K.; Staemmler, V. *Chem. Phys.* **1995**, *192*, 25.
(52) McClure, D. S. *Solid State Phys.* **1959**, *9*, 399. McClure, D. S. *J. Chem. Phys.* **1963**, *36*, 2757.
(53) Tippins, H. H. *Phys. Rev. B* **1970**, *1*, 126.

is found at 36000 cm^{-1} in the absorption spectrum of the basic rhodo ion.[28,29] It was nominally assigned as a MMCT band in ref 29, but it is probably a LMCT band as suggested in ref 54 with some MMCT character mixed in. The energy of this band is lower than the values of Δ used above. This is consistent with the fact that LMCT transitions are known to occur at lower energies upon dimer formation compared to the corresponding energy for the mononuclear fragments.[13,14,55]

5.3. The Ferromagnetic Contributions to *J*. Terms of type J_i are absent when no ligand orbital l' or linear combination of ligand orbitals simultaneously has overlaps with half-filled orbitals on the paramagnetic centers A and B. Similarly the terms J_i are absent when half-filled orbitals on the two paramagnetic centers are orthogonal by symmetry.[56,57] In these situations the terms J_{ii} and J_{iii} or true potential exchange, which we have neglected here, become important.

The fact that $|J_{ii}|$ is an order of magnitude bigger than $|J_{iii}|$ immediately tells us which transition metal electron configurations can possibly show strong net ferromagnetic interaction. We designate the d electron configuration of the metals A and B as d^{N_A} and d^{N_B}, respectively, with N_A and N_B being the total number of d electrons. If $N_A \geq 5$ and $N_B > 5$ (or vice versa) and both centers have the high-spin electron configuration, then J_{iii} is the only ferromagnetic term that can occur. This will, according to our model, lead to small ferromagnetic J_{iii} contributions to J as exemplified above with the nearest-neighbor interaction in NiO, see also eq 32. If, on the other hand, $N_A \leq 5$ and $N_B < 5$ (or vice versa) and both centers have the high-spin electron configuration, then J_{ii} are the only ferromagnetic terms present. This was exemplified with the high I/U_{eff} ratio occurring when J_{ii} is the ferromagnetic contribution to J.

For dimers in which either or both of the constituting metals have the low-spin electron configuration, both types of ferromagnetic terms J_{ii} and J_{iii} can be present. We conclude that dimers containing transition metals from the first half of the transition series will exhibit ferromagnetic interaction more frequently than dimers with metals from the second half of the transition series. A similar conclusion, based on other principles, however, was reached in ref 45, see section 5.1 of the present paper.

In summary, we have derived expressions for the contributions to the HDvV J value using a valence bond configuration interaction model. Insight into the superexchange mechanisms is obtained using perturbation theory to fourth order. An important point is the inclusion of the double LMCT configurations in the valence bond configuration interaction model. In cases i and ii it is possible to perform a double electron transfer from the ligand orbital to *both* paramagnetic centers without violating the Pauli principle. As a result, the parameter U_{eff} appearing in the old formalism for cases i and ii is strongly reduced from U due to mixing between ground and double LMCT configurations. In cases iii and iv this mixing is not possible due to the absence of double LMCT configurations involving both paramagnetic centers.

It is now possible to express the magnitude of all four contributions J_i, J_{ii}, J_{iii}, and J_{iv} to J in terms of the number of unpaired electrons, LMCT and MMCT energies, and intra-atomic exchange integrals.

Using realistic model parameters the observed trends in the exchange coupling of known transition metal ion systems can be rationalized. Reliable predictions of the magnetic properties can be made for new compounds.

Acknowledgment. This work was financially supported by the Danish and Swiss National Science Foundations.

Appendix

In this appendix we present the configuration interaction matrixes which are used in sections 4.1, 4.2, 4.3, and 4.4. We also give the difference $E(1) - E(0)$ between the energy of lowest triplet $E(1)$ and singlet $E(0)$ state of the dimer after application of fourth-order perturbation theory.[36]

A1. a_i Half-Filled and b_j Half-Filled. The basis functions $|n\rangle$ where n refers to the numbers in parentheses in Figure 1 were generated by using the following coupling schemes, see eq 15:

$$|1\rangle: \quad \left\{(a^1)\frac{1}{2} \otimes \left[(l^2)0 \otimes (b^1)\frac{1}{2}\right]\frac{1}{2}\right\}0$$

$$|2\rangle: \quad \left\{(a^1)\frac{1}{2} \otimes \left[(l^2)0 \otimes (b^1)\frac{1}{2}\right]\frac{1}{2}\right\}1$$

$$|3\rangle: \quad \left\{(a^2)0 \otimes \left[(l^1)\frac{1}{2} \otimes (b^1)\frac{1}{2}\right]0\right\}0$$

$$|4\rangle: \quad \left\{(a^2)0 \otimes \left[(l^1)\frac{1}{2} \otimes (b^1)\frac{1}{2}\right]1\right\}1$$

$$|5\rangle: \quad \left\{(a^1)\frac{1}{2} \otimes \left[(l^1)\frac{1}{2} \otimes (b^2)0\right]\frac{1}{2}\right\}0$$

$$|6\rangle: \quad \left\{(a^1)\frac{1}{2} \otimes \left[(l^1)\frac{1}{2} \otimes (b^2)0\right]\frac{1}{2}\right\}1$$

$$|7\rangle: \quad \{(a^2)0 \otimes (l^2)0\}0$$

$$|8\rangle: \quad \{(l^2)0 \otimes (b^2)0\}0$$

$$|9\rangle: \quad \{(a^2)0 \otimes (b^2)0\}0$$

The $S = 0$ configuration interaction matrix has the following form:

$$\begin{array}{c} \begin{array}{cccccc} |1\rangle & |3\rangle & |5\rangle & |7\rangle & |8\rangle & |9\rangle \end{array} \\ \left\{\begin{array}{cccccc} 0 & -V_B & -V_A & 0 & 0 & 0 \\ -V_B & \Delta_B & 0 & \sqrt{2}V_A & 0 & \sqrt{2}V_A \\ -V_A & 0 & \Delta_A & 0 & \sqrt{2}V_B & \sqrt{2}V_B \\ 0 & \sqrt{2}V_A & 0 & U_B & 0 & 0 \\ 0 & 0 & \sqrt{2}V_B & 0 & U_A & 0 \\ 0 & \sqrt{2}V_A & \sqrt{2}V_B & 0 & 0 & \Delta_{AB} \end{array}\right\} \end{array} \tag{43}$$

The $S = 1$ configuration matrix has the following form:

$$\begin{array}{c} \begin{array}{ccc} |2\rangle & |4\rangle & |6\rangle \end{array} \\ \left\{\begin{array}{ccc} 0 & -V_B & -V_A \\ -V_B & \Delta_B & 0 \\ -V_A & 0 & \Delta_A \end{array}\right\} \end{array} \tag{44}$$

To fourth order in perturbation theory we have

(54) Kahn, O.; Briat, B. *J. Chem. Soc., Faraday Trans. 2* **1976**, *72*, 268.
(55) Schugar, H. J.; Hubbard, A. T.; Anson, F. C.; Gray, H. B. *J. Am. Chem. Soc.* **1969**, *90*, 71. Reem, R. C.; McCormick, J. M.; Richardson, D. E.; Devlin, F. J.; Stephens, P. J.; Musselman, R. L.; Solomon, E. I. *J. Am. Chem. Soc.* **1989**, *111*, 4688.
(56) Kahn, O.; Galy, J.; Journaux, Y.; Jaud, J.; Morgenstern-Badarau, I. *J. Am. Chem. Soc.* **1982**, *104*, 2165.
(57) Mallah, T.; Auberger, C.; Verdaguer, M.; Veillet, P. *J. Chem. Soc., Chem. Commun.* **1995**, 61.

$$E(1) - E(0) = V_A^2 V_B^2\left[\frac{2}{\Delta_B^2 U_B} + \frac{2}{\Delta_A^2 U_A} + \frac{2}{\Delta_B^2 \Delta_{AB}} + \frac{2}{\Delta_A^2 \Delta_{AB}} + \frac{4}{\Delta_A \Delta_B \Delta_{AB}}\right] \quad (45)$$

A2. a_i Half-Filled and b_j Empty. The basis functions $|n\rangle$ where n refers to the numbers in parentheses in Figure 3 were generated by use of the following coupling schemes, see eq 15:

$|1\rangle$: $\left\{(a_1^1)\frac{1}{2} \otimes \left[(l^2)0 \otimes (b_1^1)\frac{1}{2}\right]\frac{1}{2}\right\}1$

$|2\rangle$: $\left\{(a_1^1)\frac{1}{2} \otimes \left[(l^2)0 \otimes (b_1^1)\frac{1}{2}\right]\frac{1}{2}\right\}0$

$|3\rangle$: $\left\{(a_1^1)\frac{1}{2} \otimes \left[(l^1)\frac{1}{2} \otimes (b_1^1\, b_2^1)1\right]\frac{3}{2}\right\}2$

$|4\rangle$: $\left\{(a_1^1)\frac{1}{2} \otimes \left[(l^1)\frac{1}{2} \otimes (b_1^1\, b_2^1)1\right]\frac{3}{2}\right\}1$

$|5\rangle$: $\left\{(a_1^1)\frac{1}{2} \otimes \left[(l^1)\frac{1}{2} \otimes (b_1^1\, b_2^1)1\right]\frac{1}{2}\right\}1$

$|6\rangle$: $\left\{(a_1^1)\frac{1}{2} \otimes \left[(l_1^1)\frac{1}{2} \otimes (b_1^1\, b_2^1)1\right]\frac{1}{2}\right\}0$

$|7\rangle$: $\left\{(a_1^1)\frac{1}{2} \otimes \left[(l^1)\frac{1}{2} \otimes (b_1^1\, b_2^1)1\right]\frac{1}{2}\right\}1$

$|8\rangle$: $\left\{(a_1^1)\frac{1}{2} \otimes \left[(l^1)\frac{1}{2} \otimes (b_1^1\, b_2^1)1\right]\frac{1}{2}\right\}0$

$|9\rangle$: $\left\{(a_1^1)\frac{1}{2} \otimes (b_1^1\, b_2^2)\frac{1}{2}\right\}1$

$|10\rangle$: $\left\{(a_1^1)\frac{1}{2} \otimes (b_1^1\, b_2^2)\frac{1}{2}\right\}0$

$|11\rangle$: $\left\{(a_1^2)0 \otimes \left[(l^1)\frac{1}{2} \otimes (b_1^1)\frac{1}{2}\right]1\right\}1$

$|12\rangle$: $\left\{(a_1^2)0 \otimes \left[(l^1)\frac{1}{2} \otimes (b_1^1)\frac{1}{2}\right]1\right\}0$

$|13\rangle$: $\{(a_1^2)0 \otimes (b_1^1\, b_2^1)1\}1$

$|14\rangle$: $\{(a_1^2)0 \otimes (b_1^1\, b_2^1)0\}0$

$|15\rangle$: $\{(l^2)0 \otimes (b_1^1\, b_2^1)1\}1$

$|16\rangle$: $\{[(l^2)0 \otimes (b_1^1\, b_2^1)0\}0$

The $S = 0$ matrix has the following form:

$$\begin{array}{c} \begin{array}{ccccccc} |2\rangle & |6\rangle & |8\rangle & |10\rangle & |12\rangle & |14\rangle & |16\rangle \end{array} \\ \left\{\begin{array}{ccccccc} 0 & -\sqrt{\frac{3}{2}}V_B & -\sqrt{\frac{1}{2}}V_B & 0 & -V_A & 0 & 0 \\ -\sqrt{\frac{3}{2}}V_B & \Delta_B & 0 & -\sqrt{\frac{3}{2}}V_B & 0 & 0 & 0 \\ -\sqrt{\frac{1}{2}}V_B & 0 & \Delta_B + 2I_B & -\sqrt{\frac{1}{2}}V_B & 0 & \sqrt{2}V_A & \sqrt{2}V_A \\ 0 & -\sqrt{\frac{3}{2}}V_B & -\sqrt{\frac{1}{2}}V_B & \Delta_{B2} & 0 & 0 & 0 \\ -V_A & 0 & 0 & 0 & \Delta_A & V_B & 0 \\ 0 & 0 & \sqrt{2}V_B & 0 & V_B & \Delta_{AB} + 2I_B & 0 \\ 0 & 0 & \sqrt{2}V_B & 0 & 0 & 0 & U + 2I_B \end{array}\right\} \end{array} \quad (46)$$

The $S = 1$ matrix has the following form:

$$\begin{array}{c} \begin{array}{ccccccc} |1\rangle & |4\rangle & |5\rangle & |7\rangle & |9\rangle & |11\rangle & |13\rangle & |15\rangle \end{array} \\ \left\{\begin{array}{cccccccc} 0 & 0 & -\sqrt{\frac{3}{2}}V_B & -\sqrt{\frac{1}{2}}V_B & 0 & -V_A & 0 & 0 \\ 0 & \Delta_B & 0 & 0 & 0 & 0 & \sqrt{\frac{4}{3}}V_A & \sqrt{\frac{4}{3}}V_A \\ -\sqrt{\frac{3}{2}}V_B & 0 & \Delta_B & 0 & -\sqrt{\frac{3}{2}}V_B & 0 & -\sqrt{\frac{2}{3}}V_A & -\sqrt{\frac{2}{3}}V_A \\ -\sqrt{\frac{1}{2}}V_B & 0 & 0 & \Delta_B + 2I_B & -\sqrt{\frac{1}{2}}V_B & 0 & 0 & 0 \\ 0 & 0 & -\sqrt{\frac{3}{2}}V_B & -\sqrt{\frac{1}{2}}V_B & \Delta_{B2} & 0 & 0 & 0 \\ -V_A & 0 & 0 & 0 & 0 & \Delta_A & -V_B & 0 \\ 0 & -\sqrt{\frac{4}{3}}V_A & -\sqrt{\frac{2}{3}}V_A & 0 & 0 & -V_B & \Delta_{AB} & 0 \\ 0 & -\sqrt{\frac{4}{3}}V_A & -\sqrt{\frac{2}{3}}V_A & 0 & 0 & 0 & 0 & U \end{array}\right\} \end{array} \quad (47)$$

To fourth order in perturbation theory we have

$$E(1) - E(0) = -V_A^2 V_B^2\left[\frac{1}{\Delta_B^2 U} - \frac{1}{(\Delta_B + 2I_B)^2(U + 2I_B)} + \frac{2}{\Delta_B \Delta_{AB} \Delta_A} - \frac{2}{(\Delta_B + 2I_B)(\Delta_{AB} + 2I_B)\Delta_A} + \frac{1}{\Delta_B^2 \Delta_{AB}} - \frac{1}{(\Delta_B + 2I_B)^2(\Delta_{AB} + 2I_B)} + \frac{1}{\Delta_A^2 \Delta_{AB}} - \frac{1}{\Delta_A^2(\Delta_{AB} + 2I_B)}\right] \quad (48)$$

A3. a_i Full and b_j Half-Filled. The basis functions $|n\rangle$ where n refers to the numbers in parentheses in Figure 4 were generated by use of the following coupling schemes, see eq 15.

$|1\rangle$: $\left\{(a_1^2\, a_2^1)\frac{1}{2} \otimes \left[(l^2)0 \otimes (b_1^1)\frac{1}{2}\right]\frac{1}{2}\right\}0$

$|2\rangle$: $\left\{(a_1^2\, a_2^1)\frac{1}{2} \otimes \left[(l^2)0 \otimes (b_1^1)\frac{1}{2}\right]\frac{1}{2}\right\}1$

$|3\rangle$: $\left\{(a_1^2\, a_2^1)\frac{1}{2} \otimes \left[(l^1)\frac{1}{2} \otimes (b_1^2)0\right]\frac{1}{2}\right\}0$

$|4\rangle$: $\left\{(a_1^2\, a_2^1)\frac{1}{2} \otimes \left[(l^1)\frac{1}{2} \otimes (b_1^2)0\right]\frac{1}{2}\right\}1$

$|5\rangle$: $\{(a_1^1\, a_2^1)0 \otimes [(l^2)0 \otimes (b_1^2)0]0\}0$

$|6\rangle$: $\{(a_1^1\, a_2^1)1 \otimes [(l^2)0 \otimes (b_1^2)0]1\}1$

The $S = 0$ matrix has the following form:

$$\begin{array}{c} \begin{array}{ccc} |1\rangle & |3\rangle & |5\rangle \end{array} \\ \left\{\begin{array}{ccc} 0 & -V_B & 0 \\ -V_B & \Delta & V_A \\ 0 & V_A & U + 2I_A \end{array}\right\} \end{array} \quad (49)$$

The $S = 1$ matrix has the following form:

$$\begin{array}{c} \begin{array}{ccc} |2\rangle & |4\rangle & |6\rangle \end{array} \\ \left\{\begin{array}{ccc} 0 & -V_B & 0 \\ -V_B & \Delta & V_A \\ 0 & V_A & U \end{array}\right\} \end{array} \quad (50)$$

To fourth order in perturbation theory we have

$$E(1) - E(0) = -\frac{V_A^2}{\Delta}\frac{V_B^2}{\Delta}\left[\frac{1}{U} - \frac{1}{U + 2I_A}\right] \quad (51)$$

A4. a_i Full and b_j Empty. The basis functions $|n\rangle$ where n refers to the numbers in parentheses in Figure 5 were generated

by use of the following coupling schemes, see eq 15.

$|1\rangle$: $\left\{(a_1^2\, a_2^1)\frac{1}{2} \otimes \left[(l^2)0 \otimes (b_1^1)\frac{1}{2}\right]\frac{1}{2}\right\}0$

$|2\rangle$: $\left\{(a_1^2\, a_2^1)\frac{1}{2} \otimes \left[(l^2)0 \otimes (b_1^1)\frac{1}{2}\right]\frac{1}{2}\right\}1$

$|3\rangle$: $\left\{(a_1^2\, a_2^1)\frac{1}{2} \otimes \left[(l^1)\frac{1}{2} \otimes (b_1^1\, b_2^1)0\right]\frac{1}{2}\right\}0$

$|4\rangle$: $\left\{(a_1^2\, a_2^1)\frac{1}{2} \otimes \left[(l^1)\frac{1}{2} \otimes (b_1^1\, b_2^1)0\right]\frac{1}{2}\right\}0$

$|5\rangle$: $\left\{(a_1^2\, a_2^1)\frac{1}{2} \otimes \left[(l^1)\frac{1}{2} \otimes (b_1^1\, b_2^1)1\right]\frac{1}{2}\right\}0$

$|6\rangle$: $\left\{(a_1^2\, a_2^1)\frac{1}{2} \otimes \left[(l^1)\frac{1}{2} \otimes (b_1^1\, b_2^1)1\right]\frac{1}{2}\right\}1$

$|7\rangle$: $\left\{(a_1^2\, a_2^1)\frac{1}{2} \otimes \left[(l^1)\frac{1}{2} \otimes (b_1^1\, b_2^1)1\right]\frac{3}{2}\right\}1$

$|8\rangle$: $\left\{(a_1^2\, a_2^1)\frac{1}{2} \otimes \left[(l^1)\frac{1}{2} \otimes (b_1^1\, b_2^1)1\right]\frac{3}{2}\right\}2$

$|9\rangle$: $\left\{(a_1^2\, a_2^1)\frac{1}{2} \otimes (b_1^1\, b_2^2)\frac{1}{2}\right\}0$

$|10\rangle$: $\left\{(a_1^2\, a_2^1)\frac{1}{2} \otimes (b_1^1\, b_2^2)\frac{1}{2}\right\}1$

$|11\rangle$: $\{(a_1^1\, a_2^1)0 \otimes [(l^2)0 \otimes (b_1^1\, b_2^1)0]0\}0$

$|12\rangle$: $\{(a_1^1\, a_1^2)0 \otimes [(l^2)0 \otimes (b_1^1\, b_2^1)1]1\}1$

$|13\rangle$: $\{(a_1^1\, a_2^1)1 \otimes [(l^2)0 \otimes (b_1^1\, b_2^1)0]0\}1$

$|14\rangle$: $\{(a_1^1\, a_2^1)1 \otimes [(l^2)0 \otimes (b_1^1\, b_2^1)1]1\}0$

$|15\rangle$: $\{(a_1^1\, a_2^1)1 \otimes [(l^2)0 \otimes (b_1^1\, b_2^1)1]1\}1$

$|16\rangle$: $\{(a_1^1\, a_2^1)1 \otimes [(l^2)0 \otimes (b_1^1\, b_2^1)1]1\}2$

The $S = 0$ matrix has the following form:

$$\begin{array}{c} \begin{array}{cccccc} |1\rangle & |3\rangle & |5\rangle & |9\rangle & |11\rangle & |14\rangle \end{array} \\ \left\{\begin{array}{cccccc} 0 & -\sqrt{\frac{1}{2}}V_B & -\sqrt{\frac{3}{2}}V_B & 0 & 0 & 0 \\ -\sqrt{\frac{1}{2}}V_B & \Delta_B + 2I_B & 0 & -\sqrt{\frac{1}{2}}V_B & -V_A & 0 \\ -\sqrt{\frac{3}{2}}V_B & 0 & \Delta_B & -\sqrt{\frac{3}{2}}V_B & 0 & V_A \\ 0 & -\sqrt{\frac{1}{2}}V_B & -\sqrt{\frac{3}{2}}V_B & \Delta_{B2} & 0 & 0 \\ 0 & -V_A & 0 & 0 & U + 2I_A + 2I_B & 0 \\ 0 & 0 & V_A & 0 & 0 & U \end{array}\right\} \end{array} \quad (52)$$

The $S = 1$ matrix has the following form:

$$\begin{array}{c} \begin{array}{cccccccc} |2\rangle & |4\rangle & |6\rangle & |7\rangle & |10\rangle & |12\rangle & |13\rangle & |15\rangle \end{array} \\ \left\{\begin{array}{cccccccc} 0 & -\sqrt{\frac{1}{2}}V_B & -\sqrt{\frac{3}{2}}V_B & 0 & 0 & 0 & 0 & 0 \\ -\sqrt{\frac{1}{2}}V_B & \Delta_B + 2I_B & 0 & 0 & -\sqrt{\frac{1}{2}}V_B & 0 & V_A & 0 \\ -\sqrt{\frac{3}{2}}V_B & 0 & \Delta_B & 0 & -\sqrt{\frac{3}{2}}V_B & \sqrt{\frac{1}{3}}V_A & 0 & \sqrt{\frac{2}{3}}V_A \\ 0 & 0 & 0 & \Delta_B & 0 & -\sqrt{\frac{2}{3}}V_A & 0 & \sqrt{\frac{1}{3}}V_A \\ 0 & -\sqrt{\frac{1}{2}}V_B & -\sqrt{\frac{3}{2}}V_B & 0 & \Delta_{B2} & 0 & 0 & 0 \\ 0 & 0 & \sqrt{\frac{1}{3}}V_A & -\sqrt{\frac{2}{3}}V_A & 0 & U + 2I_A & 0 & 0 \\ 0 & V_A & 0 & 0 & 0 & 0 & U + 2I_B & 0 \\ 0 & 0 & \sqrt{\frac{2}{3}}V_A & \sqrt{\frac{1}{3}}V_A & 0 & 0 & 0 & U \end{array}\right\} \end{array} \quad (53)$$

To fourth order in perturbation theory we have

$$E(1) - E(0) = {}^1/_2 V_A^2\, V_B^2 \left[+ \frac{1}{\Delta_B^2 U} + \frac{1}{(\Delta_B + 2I_B)^2 (U + 2I_A + 2I_B)} - \frac{1}{\Delta_B^2 (U + 2I_A)} - \frac{1}{(\Delta_B + 2I_B)^2 (U + 2I_B)} \right] \quad (54)$$

IC990779H